

# Synthesis, Characterization And Larvicidal Activity Of Schiff Base Ligand 5-(((5-mercapto- 1,3,4-thiadaizol-2-yl)imino)methyl)-2-methoxyphenol And Its Metal(Ii) Complexes

P Deepika

JSS Science and Technology University

Vinusha H. M

Sarada Vilas College

Muneera Begum (✉ [mbegum20@yahoo.com](mailto:mbegum20@yahoo.com))

JSS Science and Technology University

N D Rekha

JSS College of Arts, Commerce and Science (Autonomous)

---

## Research Article

**Keywords:** Schiff base transition metal complexes, spectroscopic studies, larvicidal bioassay

**Posted Date:** June 22nd, 2022

**DOI:** <https://doi.org/10.21203/rs.3.rs-1737417/v1>

**License:** © ⓘ This work is licensed under a Creative Commons Attribution 4.0 International License.

[Read Full License](#)

---

# Abstract

In the current work we have synthesized a Schiff base ligand 5-(((5-mercapto-1,3,4-thiadaizol-2-yl)imino)methyl)-2-methoxyphenol (HL) derived from the condensation of 5-amino-1,3,4-thiadaizole 2-thiol and 3-hydroxy-4-methoxy benzaldehyde and its Cu(II), Mn(II) and Zn(II) metal complexes in 2:1 stoichiometric ratio (2HL:M). The formation of the ligand and its metal complexes were evaluated using MS technique, FT-IR, UV-Visible,  $^1\text{H-NMR}$ ,  $^{13}\text{C-NMR}$  and thermogravimetric analysis. The larvicidal bioassay were also done for all the metal complexes and Schiff base ligand. The mortality of the larvicidal activity were also determined.

## Introduction

Schiff base ligand is a compound prepared by the condensation reaction between aldehyde or ketone with a primary amine [1–2]. The product group is called azomethine group  $-\text{HC} = \text{N}-$ . The Schiff base complexes can be prepared by the reaction between the ligand and the metal salts. The active groups in the compounds play an important role in its applications. The Schiff base and its complexes have innumerable applications according to the active groups.

Schiff bases are considered to be notable ligands for metal ion coordination complexes due to their ease of synthesis, variability in structural design, and wide range of applications [3–7]. Chemists design Schiff bases as polydentate ligands and their complexes have served several areas of chemistry. These ligands were broadly used as polychelator ligands and have revealed high performance in terms of steric characteristics and electronic soft tuning of their metal complexes [8–13].

Literature survey for Schiff base metal complexes and their applications showed excellent review articles [14–15] for the detailed understanding of this class of compounds in all respects [16]. They provide several details on number of metal complexes derived from Schiff bases used widely for applications in food and dye industry [17], analytical chemistry [18], catalysis [19], polymers [20], antifertility [21], agrochemical [22], anti-inflammatory activity [23], antiradical activities [24], and biological systems as enzymatic agents [25]. Several Schiff base metal compounds exhibits antimicrobial [26], antibacterial [27], antifungal [28], antitumor [29] and cytotoxic activities [30].

Schiff base ligands have significant importance in inorganic chemistry, especially in the development of Schiff base metal complexes, many Schiff base complexes show excellent catalytic activity in various reaction at high temperature and in the presence of moisture. Over the past few years, there have been many reports on their applications in homogeneous and heterogeneous catalysis.

Considering the above applications, in the present research study, we have synthesized a Schiff base ligand by the condensation of equivalent amount of 5-amino-1,3,4-thiadaizole 2-thiol and 3-hydroxy-4-methoxy benzaldehyde and and its Cu(II), Mn(II) and Zn(II) metal complexes in 2:1 stoichiometric ratio (2HL:M). The synthetic details of Schiff base ligand, its respective complexes, their spectral characterization and also, larvicidal studies of synthesized compounds were discussed.

# Experimental Section

## 2.1 Materials and Methods

5-amino-1,3,4-thiadiazole 2- thiol and 3-hydroxy-4-methoxy benzaldehyde were purchased from Sigma Aldrich. All the metal salts and solvents used in this work were purchased from Merck chemical company and used as received. The completion of a reaction was monitored by using thin layer chromatography (TLC) made on pre-coated silica gel plates (Merck).

Mass spectra were recorded on an Agilent technologies (HP) 5973 mass spectrometer operating at an ionization potential of 70 eV. The  $^1\text{H}$  and  $^{13}\text{C}$ -NMR spectra were recorded with a Varian 300 MHz in  $\text{DMSO-d}_6$  as a solvent against tetramethylsilane as an internal standard. Infrared spectra were recorded on a Perkin Elmer FT-IR type 1650 spectrophotometer in the region  $4000 - 400 \text{ cm}^{-1}$  using KBr pellets. The electronic absorption spectra were recorded using UV-1800 spectrophotometer (Shimadzu). Thermogravimetric analysis (TGA) was carried out on a Universal TGA Q50 instrument at a heating rate of  $2^\circ\text{C}/\text{min}$  between 30 and  $1000^\circ\text{C}$ .

## 2.2 Larvicidal bioassay:

In 1930, Weindling first discovered the genus *Trichoderma* spp. as a biocontrol agent and since then numerous studies have demonstrated that *Trichoderma* is an effective biocontrol agent for phytopathogenic microorganisms. In the current experiment, *Trichoderma* is preventing the growth of *F.oxysporum*. Further, the micronutrients are enhancing the growth of the *Trichoderma* at 15ppm concentration and inhibiting the growth of *F.oxysporum*.

Laboratory bioassay were carried out to evaluate the effect of inorganic metal complexes on *Tribolium confusum* (Coleoptera:Tenebrionidae), stored grain pests.

The purpose of bioassay is to determine the effect of a given agent on the physiology of an organism, which is generally associated with determining the toxicity of a chemical compound or resistance to it. Here in our investigation, we followed the petridish method. In this method, the bottom of the petriplates was covered with Whattman no.1 filter paper and sprayed with different metal nanoparticles and allowed to dry for around 30 min at room temperature. After this, the larvae of the *Tribolium confusum* (Six numbers to each petriplate) were transferred to the dishes using a fine brush. Mortality rate was measured after 24 hrs. and 48 hrs. suitable controls were maintained. Mortality was recorded after 24 h of exposure.

Larvae were considered dead when they were moribund or failed to do any movement. The dead larvae were counted, and the average percentage mortality was calculated. Data were adjusted for control mortality using Abbott's formula.

$$\text{Mortality (\%)} = \frac{X-Y}{X} \times 100$$

Where X was the percentage of survival in the control larvae population and Y was the percentage survival in the treated larvae population. The same formula was applied to both laboratory and wild larvae population. Lethal dosages killing 50% (LC50) and 95% (LC95)

The product *Trichoderma* is collected from the Agri-horticulture college in Mysore. This product powder of the *Trichoderma* dissolved in water without clumps. The liquid was centrifuged for 15 minutes at 3000rpm, supernatant and residue were separated from the liquid. This separated component was kept in refrigerator for a while. The contents were swabbed separately on potato dextrose agar media [31–32]. *Fusarium oxysporum* was collected from Dept. of Microbiology, University of Mysore.

## 2.3 *Trichoderma* antagonism against *Fusarium oxysporum* coinidia

The assay for antagonism was performed on Potato Dextrose Agar (PDA) by incorporating 100µg/15ml of PDA on Petri dishes by the dual culture method. The mycelial plugs (5mm diameter) of 5 day old fungal antagonist (*Trichoderma*) and the pathogen *F.oxysporum* were placed on the same petriplate with a distance of 6cm from each other. Paired cultures were incubated at room temperature (30 ± 5°C) for 192 hours. Petriplates inoculated only with test pathogens served as controls. The experiment was conducted in triplicates.

Growth was calculated using the formula:

$$\% \text{ inhibition} = \frac{\text{Control} - \text{Test}}{\text{Control}} \times 100$$

C = Average increase in mycelial growth in control plates

T = Average increase in mycelial growth in treatment plate.

## 2.4 Synthesis of 5-(((5-mercapto-1,3,4-thiadaizol-2-yl)imino)methyl)-2-methoxyphenol (HL)

The Schiff base ligand (HL) was synthesized by condensing an ethanolic solution of 5-amino-1,3,4-thiadaizole 2- thiol and 3-hydroxy-4-methoxy benzaldehyde in 1:1 molar ratio. Under reflux, the reaction mixture was stirred for 6 hours. TLC was used to monitor the completion of reaction. The precipitate obtained was filtered, washed with ethanol and dried. Recrystallization from hot ethanol yields a ligand.

## 2.5 Synthesis of metal complexes

The Cu(II), Mn(II) and Zn(II) Schiff base complexes were synthesized with the addition of aqueous metal salt solutions to a methanolic solution of Schiff base ligand in 1:2 ratio (1M:2HL). The resulting mixtures were refluxed for 2h upon which the complexes were precipitated. The obtained precipitate was filtered which was then washed with ethanol, recrystallized with hot ethanol, and dried.

## Results And Discussion

## 3.1 Reaction Scheme of ligand

## 3.2 Mass spectroscopy

The mass spectrum of the Schiff base ligand was recorded and observed for the confirmation of synthesized ligand. Figure 1 shows the mass spectrum of the synthesized ligand. The molecular ion peak of the ligand was observed at 267.95 which corresponds to the molecular weight of ligand. This confirms the formation of Schiff base ligand. Figures 2, 3 and 4 shows the mass spectra of Cu(II), Mn(II) and Zn(II) complexes. The molecular ion peak for Cu(II), Mn(II) and Zn(II) complexes was observed at  $m/z = 593.33$ , 585.21 and 595.22 respectively. It indicates the co-ordination of Cu, Mn and Zn ions with the ligand.

## 3.3 NMR spectroscopy

The  $^1\text{H}$  and  $^{13}\text{C}$ -NMR spectra of Schiff base ligand (HL) were recorded in DMSO- $d_6$ . The  $^1\text{H}$ -NMR spectrum of ligand is shown in Fig. 5. The singlet peak at  $\delta = 9.522$  ppm corresponds to azomethine group which confirms the formation of imine bond in a ligand. The peaks between  $\delta = 6.437$  and 7.449 ppm were attributed to the aromatic protons present in the ligand. The peaks at  $\delta = 3.851$  ppm were due to methoxy proton present in a ligand.

Similarly, the peak seen in ligand at  $\delta = 161.543$  ppm supports the existence of the azomethine group, as shown in Fig. 6. Carbon of the methoxy group ( $-\text{OCH}_3$ ) was found at  $\delta = 57.140$  ppm. Between  $\delta = 113.433$  and 155.161 ppm, aromatic ring carbon signals were detected. The synthesis of the reported ligand, is therefore confirmed by  $^1\text{H}$  and  $^{13}\text{C}$ -NMR findings.

## 3.4 IR spectra

Figure 7, 8, 9 and 10 shows the FT-IR spectra of the synthesized ligand and its Cu(II), Mn(II) and Zn(II) complexes. The formation of ligand and its complexes with respective metals has been confirmed by detecting the peaks of C = N groups. In ligand, the peak was found at stretching frequency of  $1631\text{ cm}^{-1}$  indicates the formation of imine bond in the ligand. But this peak was shifted to lower/higher values in the case of metal complexes due to coordination. Therefore, the peaks of C = N groups were observed at stretching frequencies of  $1601\text{ cm}^{-1}$  to  $1612\text{ cm}^{-1}$  for Cu(II), Mn(II) and Zn(II) complexes respectively.

Meanwhile, the peak of metal-nitrogen (M-N), metal-oxygen (M-O) and metal-sulfur (M-S) bonds, has verified the formation of metal complexes. For Cu(II), Mn(II) and Zn(II), M-N bonds were detected at 416 to  $476\text{ cm}^{-1}$  respectively. The M-O bonds were observed at 588 to  $609\text{ cm}^{-1}$ . The M-S bonds were  $370\text{ cm}^{-1}$  to  $383\text{ cm}^{-1}$  [33–34]. The existence of these peaks, which are completely absent in the spectrum of HL ligand as given in Table 1, further supports the formation of metal complexes.

## 3.5 Electronic Spectra

The electronic spectra of ligand and its metal complexes were recorded in DMSO solution at room temperature was shown in Figs. 11,12,13 and 14. The absorption bands around 331 and 375 nm were

observed in the spectrum of the free Schiff base ligand, corresponds to  $\pi \rightarrow \pi^*$  and  $n \rightarrow \pi^*$  transitions associated with benzene rings and azomethine groups respectively. In the metal complexes  $\pi \rightarrow \pi^*$  and  $n \rightarrow \pi^*$  transitions were shifted to longer wavelengths as a consequence of coordination to metal in Table 2, confirming the formation of Schiff base metal complexes [35–36].

### 3.6 Thermal property

The thermal property of the complexes was studied by TGA and DTG studies. Figures 15, 16 and 17 shows the TGA and DTG curves of Cu(II), Mn(II) and Zn(II) complexes under nitrogen atmosphere. From the TGA curves it is clear that of Cu(II), Mn(II) and Zn(II) complexes undergo decomposition in three steps and leaving a residue as their respective metal oxides. The step wise decomposition of all the metal complexes was given in a Table 3.

The results revealed that Cu(II) complex undergo decomposition in three steps. In the first step from 33.25–173.01 °C with the weight loss of 10.01%. In the second step, between the range 173.01–253.56 °C with weight loss of 19.60% corresponds to the loss of organic moiety of a ligand and in the third step of decomposition between 253.56–673.03 °C with a weight loss of 29.71% corresponding to the Schiff base ligand leaving with 40.68% residue as CuO.

Similarly, the results also revealed that Mn(II) complex undergo decomposition in three steps. In the first step from 28.98–215.51 °C with the weight loss of 11.79%. In the second step, between the range 215.51–315.09 °C with weight loss of 22.13% corresponds to the loss of organic moiety of a ligand and in the third step of decomposition between 315.09–685.66 °C with a weight loss of 30.73% corresponding to the Schiff base ligand leaving with 35.35% residue as MnO.

Similarly, the results also revealed that Zn(II) complex undergo decomposition in three steps. In the first step from 26.85–195.24 °C with the weight loss of 10.93%. In the second step, between the range 195.24–299.08 °C with weight loss of 20.19% corresponds to the loss of organic moiety of a ligand and in the third step of decomposition between 299.08–646.54 °C with a weight loss of 31.13% corresponding to the Schiff base ligand leaving with 37.75% residue as ZnO.

### 3.7 Larvicidal bioassay

Approximately 384 larvae were used to test the toxicity of synthesized Schiff base ligand and its metal complexes. The difference in the mortality among the different compounds is because of the nature of metal. Here we showed the pronounced larvicidal activity of the inorganic metal complexes, of which Cu(II) metal complex have potent larvicidal activity with survival rate ranging from (35%), followed by Schiff base ligand with approximately 50% larvicidal activity as shown in Figs. 18 and 19. Percentage of survival activity was shown in Table 4.

#### Mechanism of biocontrol of *Trichoderma* against *Fusarium oxysporum*

The natural method of eliminating and controlling the insects, pests and other disease-causing agents using their natural, biological enemies is called biocontrol or biological control. The agents which are employed for this are called biocontrol agents. Microbes are one of them. Biocontrol works on the principle of predation and parasitism. Bio controlling method is healthier than killing insects and pests using insecticides and pesticides. Thus, this prevents soil pollution and health issues related to insecticide poisoning, etc.

Plant diseases play a direct role in the destruction of natural resources in agriculture. In particular, soil-borne pathogens cause important losses, fungi being the most aggressive. The distribution of several phytopathogenic fungi, such as *Phythium*, *Phytophthora*, *Botrytis*, *Rhizoctonia* and *Fusarium* have spread with detrimental effects on crops of economic importance. Several modes of action of microbial biocontrol agents have been identified, none of which are mutually exclusive. These can involve interactions between the antagonist and pathogen directly, either associated with roots or seeds, or free in the soil. Soil borne plant pathogenic fungi cause heavy crop losses all over the world. Chemical control of such plant pathogens disturbs the environment, subverts ecology, degrades soil productivity, and mismanages water resources. Biocontrol agent (BCAs) can inhibit the growth of soil borne pathogens through various biocontrol mechanisms such as ability to grow much faster than them for space and nutrients, producing many powerful plant degrading enzymes such as lytic enzymes, proteolytic enzymes and more than 200 types of antibiotics which are highly toxic to any macro- and microorganism. The role of *Trichoderma* species is not only to control the growth of pathogenic microbes, but there are various other uses for *Trichoderma* species such as, enhance plant defense responses, stimulate colonization of rhizosphere and stimulates plant growth, root growth.

### **3.8 Antagonistic potential of *T. harzianum* against *F. oxysporum* in vitro**

The antagonistic potential of *T. harzianum* against *F. Oxysporum* showed increased in

Inhibition of *F. oxysporun*, after seven days of incubation in the dual culture method. The control plates which were not inoculated with *T. harzianum* but containing only *F. oxysporum* grew much faster when compared with *F. oxysporum* in the dual culture plates. The petriplates which have been incorporated with different metal complexes also enhanced the growth of *T. harzianum* and inhibited the growth of *F. oxysporum*. The role of different metal complexes in enhancing the growth of *T. harzianum* and thereby inhibiting the growth of *F. oxysporum* is as given in the Table 5. Among all the compounds Mn(II) shows best which enhances the growth of *Trichoderma* followed by Cu(II) and Zn(II) and Schiff base ligand.

## **Conclusion**

To sum up, we have synthesized 5-(((5-mercapto-1,3,4-thiadaizol-2-yl)imino)methyl)-2-methoxyphenol (HL) and its Cu(II), Co(II) and Zn(II) complexes. The reported compounds were confirmed by using various spectral techniques. All the compounds were evaluated for Larvicidal bioassay. The study reveals that larvicidal activity Cu(II) metal complex have potent larvicidal activity with survival rate ranging from

(35%), followed by Schiff base ligand with approximately 50% larvicidal activity. Among all the compounds Mn(II) shows best which enhances the growth of Trichoderma followed by Cu(II), Zn(II) and Schiff base ligand.

## Declarations

### Acknowledgements

The authors greatly thank TEQIP-III, NPIU, Sri Jayachamarajendra College of Engineering, JSS Science & Technology University, Mysuru for providing financial support and instrumentation facility.

### Conflicts of Interest

The authors declare no conflict of interest.

## References

1. Y. Gutha, Y. Zhang, W. Zhang, X.Jiao. *Int. J. Biol. Macromol* **97**, 85–98 (2017)
2. E.M.S. Azzam, G. Eshaq, A.M. Rabie, A.A. Bakr, A.A. Abd-Elaal, A.E. El Metwally, S.M. Tawfik, *Int. J. Biol. Macromol.* **89**, 507–517 (2016)
3. S.M. Bensaber, H. Allafe, N.B. Ermeli, S.B. Mohamed, A.A. Zetrini, S.G. Alsabri, M. Erhuma, A. Hermann, M.L. Jaeda, A.M. Gbaj. *Med. Chem. Res.* **23**, 5120–5134 (2014)
4. R.Udupi. *J. Chem. Pharm. Research.* **4**, 1151–1159 (2012)
5. L. Jia, J. Xu, X. Zhao, S. Shen, T. Zhou, Z. Xu, T. Zhu, R. Chen, T. Ma, J. Xie, J. J. *Inorg. Biochem.* **159**, 107–119 (2016)
6. K.S. Kumar, S. Ganguly, R. Veerasamy, E. De Clercq, *Eur. J. Med. Chem.* **45**, 5474–5479 (2010)
7. Z. Shokohi-Pour, H. Chiniforoshan, A.A. Momtazi-Borojeni, B. Notash. *J. Photochem. Photobiol. B: Boil.* **162**, 34–44 (2016)
8. P.A. Vigato, S. Tamburini, *Co-ord. Chem. Rev.* **248**, 1717–2128 (2004)
9. P.R. Inamdar, R. Chauhan, J. Abraham, A Sheela *Inorg. Chem. Commun.* **67**, 67–71 (2016)
10. I. Warad, A. Khan, M. Azam, S. Al-Resayes, T. Haddad, *J. Mol. Struct.* **1062**, 167–173 (2014)
11. M. Azam, I. Warad, S. Al-Resayes, M. Shakir, M. Ullah, A. Ahmad, F.H. Sarkar, *Inorg. Chem. Commun.* **20**, 252–258 (2012)
12. M. Azam, Z. Hussain, I. Warad, S.I. Al-Resayes, M.S. Khan, M. Shakir, A. Trzesowska-Kruszynska, R. Kruszynski. *Dalton Trans.* **41**, 10854–10864 (2012)
13. R. Jain, B. Ahuja, B. Sharma, *Indian J. Pure Appl. Phys.* **42**, 43–48 (2004)
14. W. Qin, S. Long, M. Panunzio, B. Stefano. *Molecules.* **18**, 10, 12264–12289 (2013)
15. S. Kumar, D.N. Dhar, P. N. Saxena. *Sci Ind Res.* **68**, 3, 181–187 (2009)
16. R. Katwal, H. Kaura, B.K. Kapur, *Sci. Rev. Chem. Commun.* **3**(1), 1–15 (2013)

17. V.S.S. Rani, T. Dhanasekaran, M. Jayathuna, V. Narayanan, D. Jesudurai. *Materials Today: Proceedings*, 5, 2, 8784–8788 (2018)
18. A. Sakthivel, K. Jeyasubramanian, B. Thangagiri, J.D. Raja, J. Mol. Struct. 128885 (2020)
19. K. Gupta, A.K. Sutar, Coord. Chem. Rev. **252**, 12–14 (2008) 1420–1450
20. T. Kaliyappan, S. Rajagopan, P. Kannan. (2004). *J. Appl. Polym. Sci.* 91,1, 494–500 (2004)
21. Z. Gong, L. Qian, S. Shao, B. Fan, J. Peng, K. Lu, S. Gao. *J. Chem. Eng.* **436**, 135034 (2022)
22. D.R. Gayakwad, S.R. Sarda, R.B. Nawale, S.B. Munde, J.V. Bharad, P.S. Kendrekar nt. *J. Curr. Pharm. Res.* **9**, 4, 3378–3385 (2019)
23. M. Azam, S.I. Al-Resayes, A. Trzesowska-Kruszynska, R. Kruszynski, F. Shakeel, S.M. Soliman, S.M. Wabaidur, J. Mol. Struct. **1201**, 127177 (2020)
24. N. Turan, A. Savci, K. Buldurun, Y. Alan, R. Adigüzel, Lett. Org. Chem. **13**, 5, 343–351 (2016)
25. P. Nunes, Y. Yildizhan, Z. Adiguzel, F. Marques, J. Costa Pessoa, C. Acilan, I. Correia. *J. Biol. Inorg. Chem.* **27**, 1, 89–109 (2022)
26. C. Shiju, D. Arish, S. Kumaresan. *J. Mol. Struct.* **1221**, 128770 (2020)
27. H. Kargar, A.A. Ardakani, M.N. Tahir, M. Ashfaq, K.S. Munawar, *J. Mol. Struct.* **1233**, 130112 (2021)
28. L. Wei, J. Zhang, W. Tan, G. Wang, Q. Li, F. Dong, Z. Guo, *Int. J. Biol. Macromol.* **179**, 292–298 (2021)
29. W.H. Mahmoud, R.G. Deghadi, G.G. Mohamed, *Appl. Organomet. Chem.* **30**, 4, 221–230 (2016)
30. A. Sakthivel, K. Jeyasubramanian, B. Thangagiri, J.D. Raja, *J. Mol. Struct.* 128885 (2020)
31. J. Saranya, S.S. Lakshmi, *J. Chem. Pharm.* **7**, 4, 180–186 (2015)
32. S.S. Lakshmi, K. Geetha, P. Mahadevi, *J. Chem. Sci.* **128**, 7, 1113–1118 (2016)
33. E. Erdem, E.Y. Sari, R. Kiliñarslan, N. Kabay, *Transit. Met. Chem.* **34**, 2, 167–174 (2009)
34. A.E.M.M. Ramadan, S.Y. Shaban, M.M. Ibrahim, M.M. El-Hendawy, H. Eissa, S.A. Al-Harbi, *J. Chin. Chem. Soc.* **67**,1, 135–151 (2020)
35. N. Beyazit, D. Çakmak, C. Demetgül. *Tetrahedron* **73**(19), 2774–2779 (2017)
36. I.T. Ahmed, *Spectrochim Acta- Part A: Mol. Biomol. Spectrosc.* **65**, 1, 5–10 (2006)

## Tables

**Table 1** IR spectral data of ligand and its metal complexes in  $\text{cm}^{-1}$ .

Compound	OH	-C=N	C=C	O-CH <sub>3</sub>	M-O	M-N	M-S
Schiff base ligand (HL)	3185	1631	1560	1488	-	-	-
Cu(II)	-	1608	1534	1437	588	416	383
Mn(II)	-	1612	1546	1472	607	476	379
Zn(II)	-	1601	1528	1444	609	448	370

**Table 2** Electronic absorption spectral data of ligand and its metal complexes in nm.

Compound	$\pi-\pi^*$	$n-\pi^*$
HL	331	375
HL - Cu	335	390
HL - Mn	345	395
HL - Zn	340	387

**Table 3** Stepwise thermal decomposition of metal complexes.

Compounds	Stages	Range	Weight Loss (%)	Residue (%)
HL - Cu	I	33.25 - 173.01	10.01	40.68
	II	173.01 - 253.56	19.60	
	III	253.56 - 673.03	29.71	
HL - Mn	I	28.98 - 215.51	11.79	35.35
	II	215.51 - 315.09	22.13	
	III	315.09 - 685.66	30.73	
HL - Zn	I	26.85 - 195.24	10.93	37.75
	II	195.24 - 299.08	20.19	
	III	299.08 - 646.54	31.13	

**Table 4** % of survival larvicidal activity

Name of the chemical compound	% Survival
D2 Ligand	55%
D2 Cu	35%
D2 Zn	67%
D2 Mn	78%

**Table 5** % Increase in the growth of Trichoderma over Fusarium oxysporum

Name of the compounds	% Increase in the growth of Trichoderma over Fusarium oxysporum
D2 ligand	53.33
D2 Cu	86
D2 Mn	133
D2 Zn	67

## Scheme 1

Scheme 1 is available in the Supplementary Files section.

## Figures

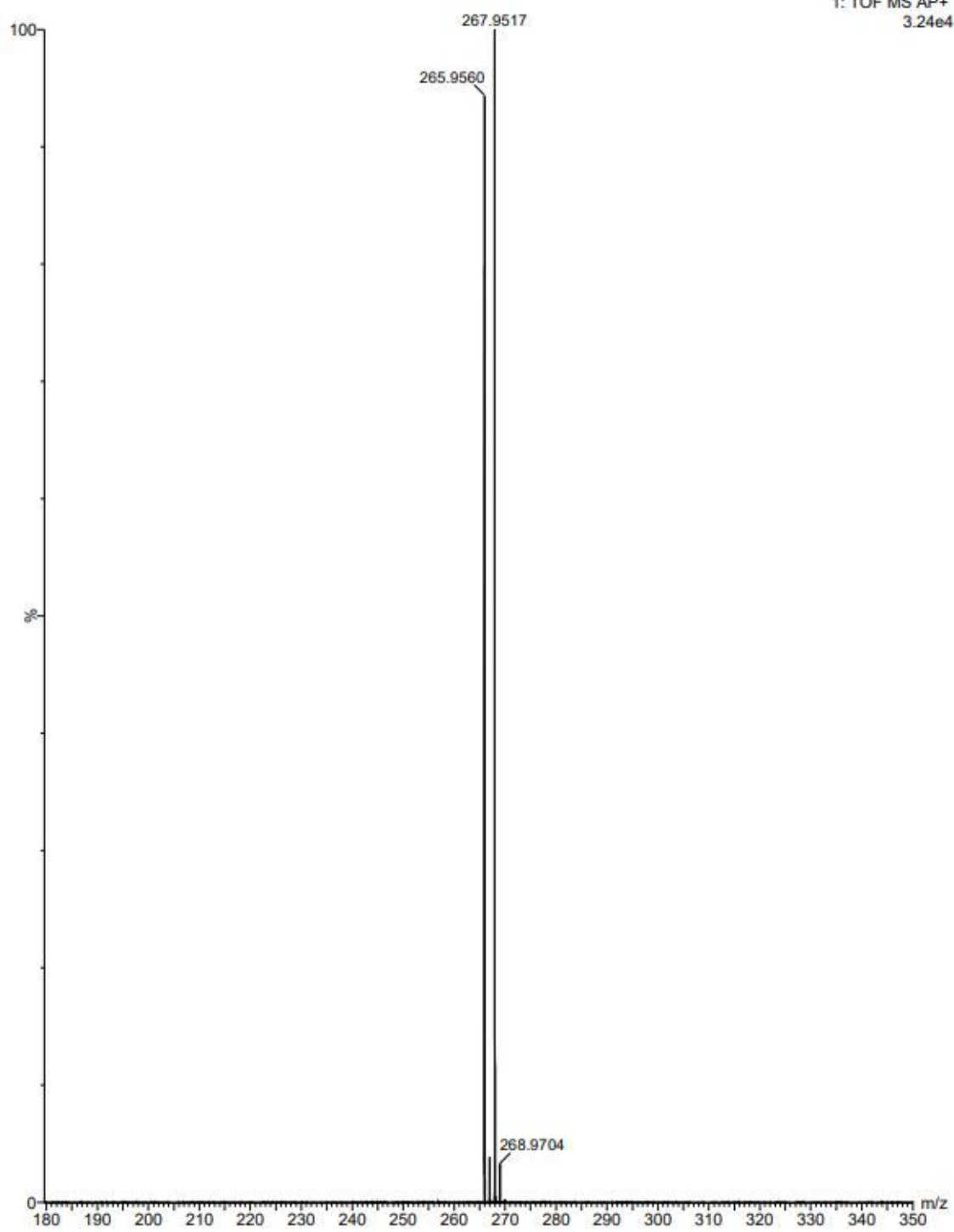


**Figure 1**

Mass spectrum of the Schiff base ligand.

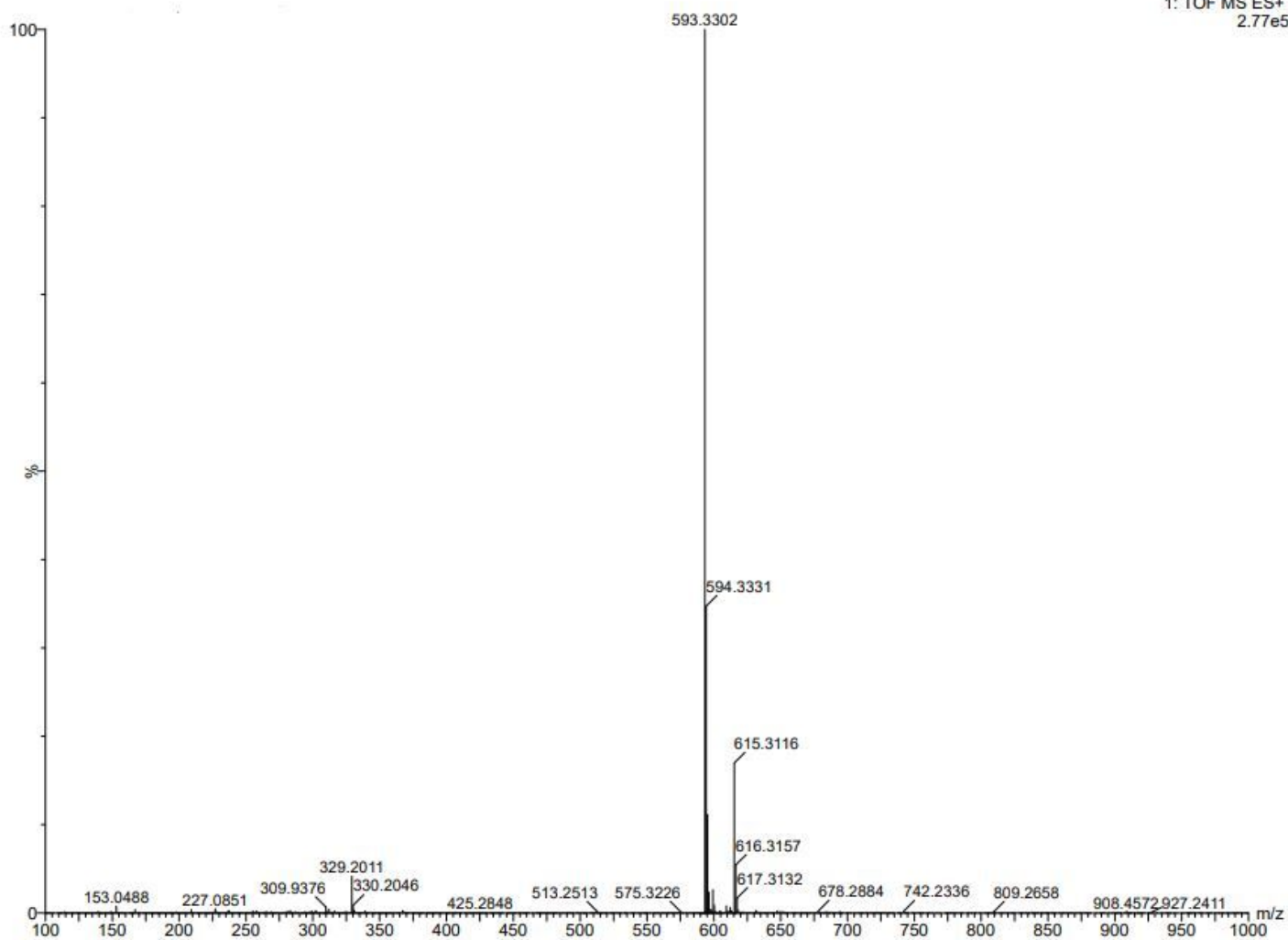


**Figure 2**

Mass spectrum of the Cu(II) complex.

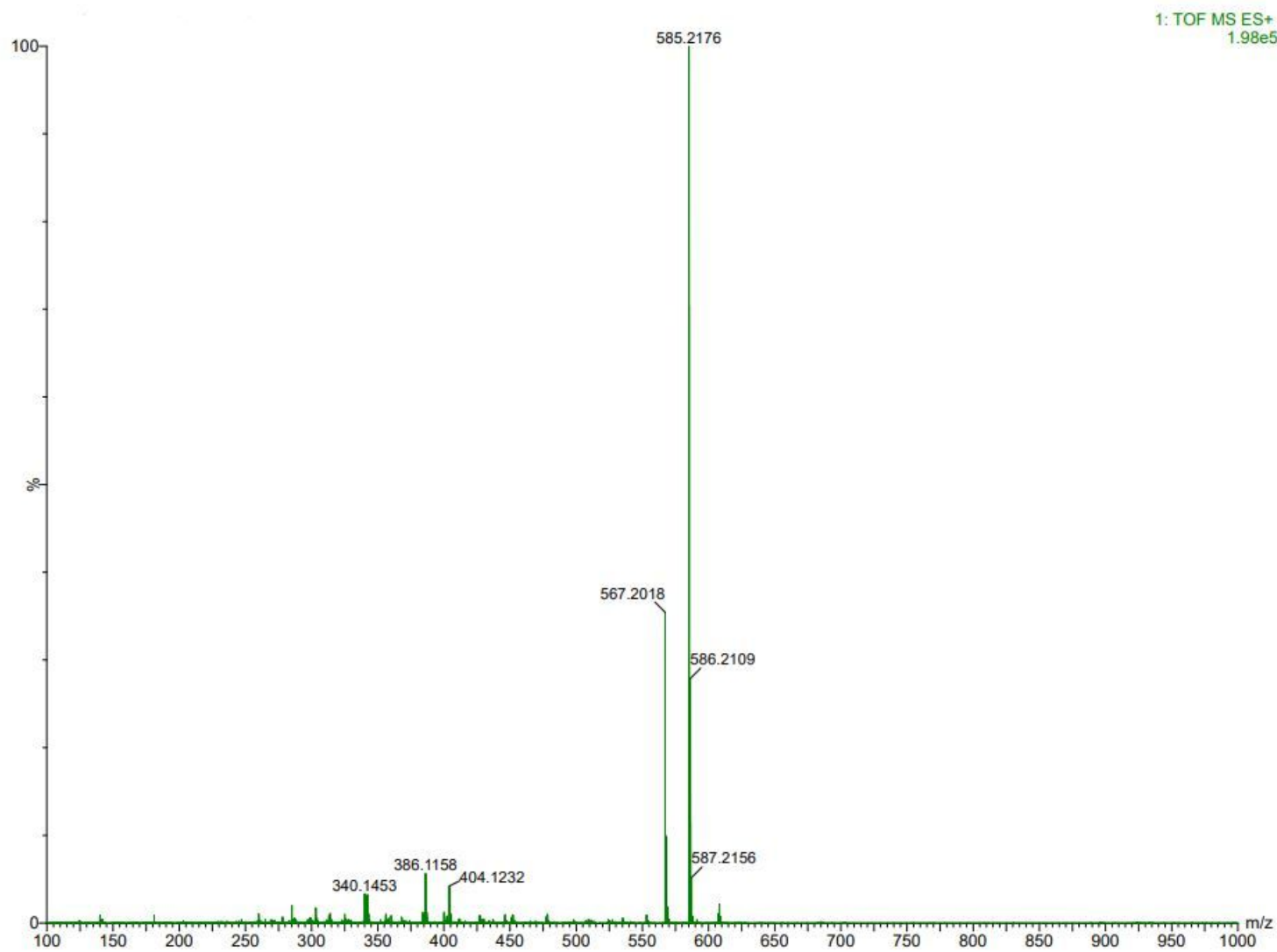


**Figure 3**

Mass spectrum of the Mn(II) complex.

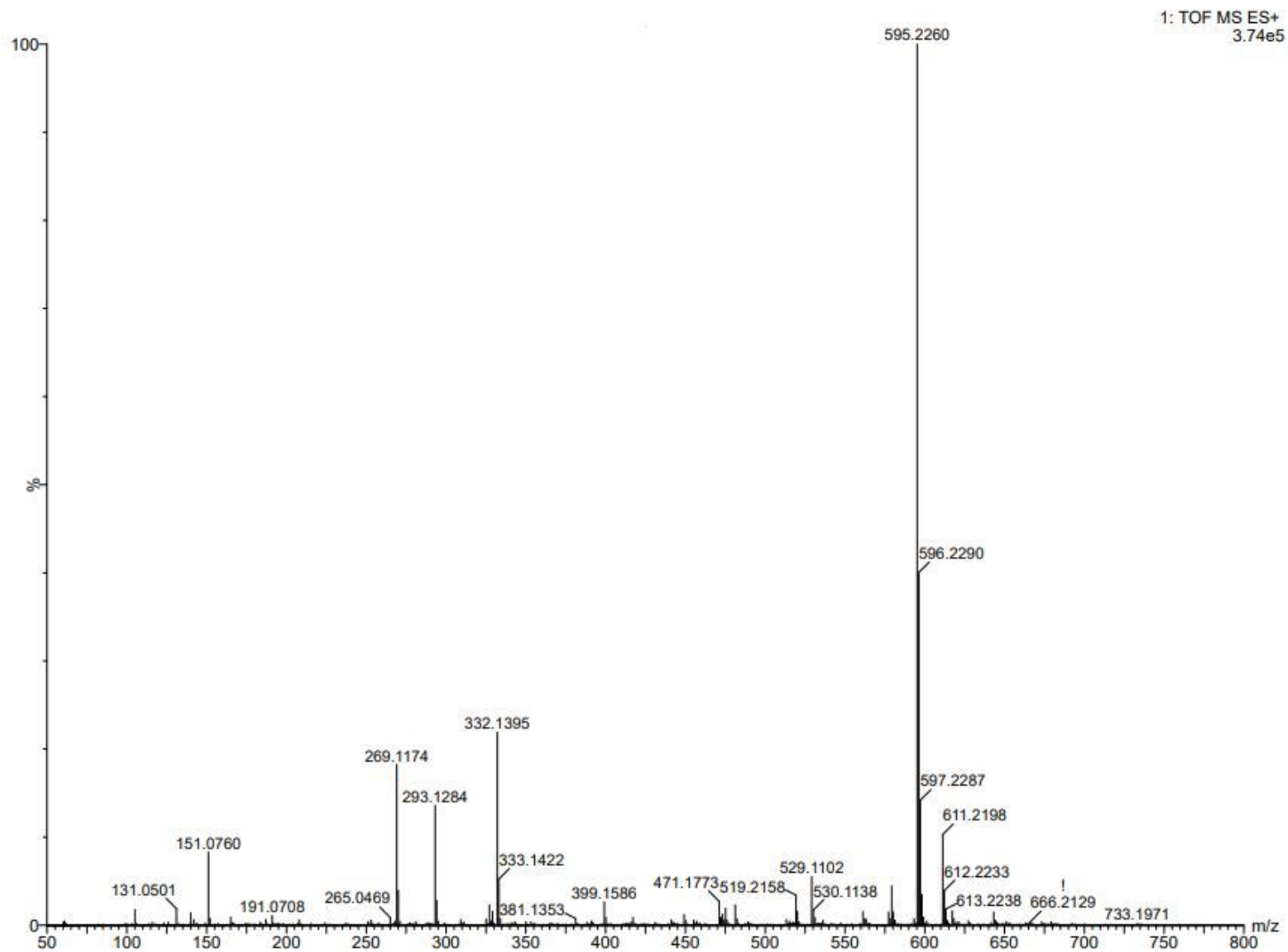


**Figure 4**

Mass spectrum of the Zn(II) complex.

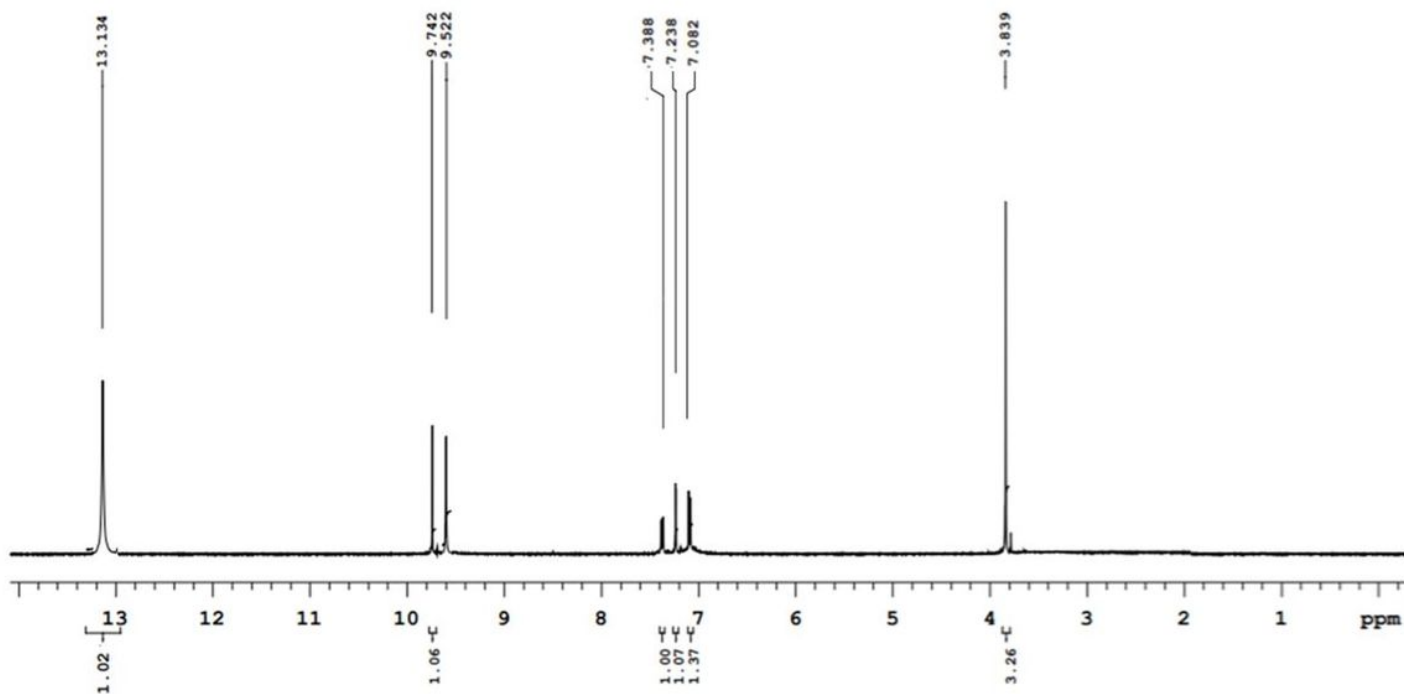


Figure 5

<sup>1</sup>H NMR spectrum of ligand.

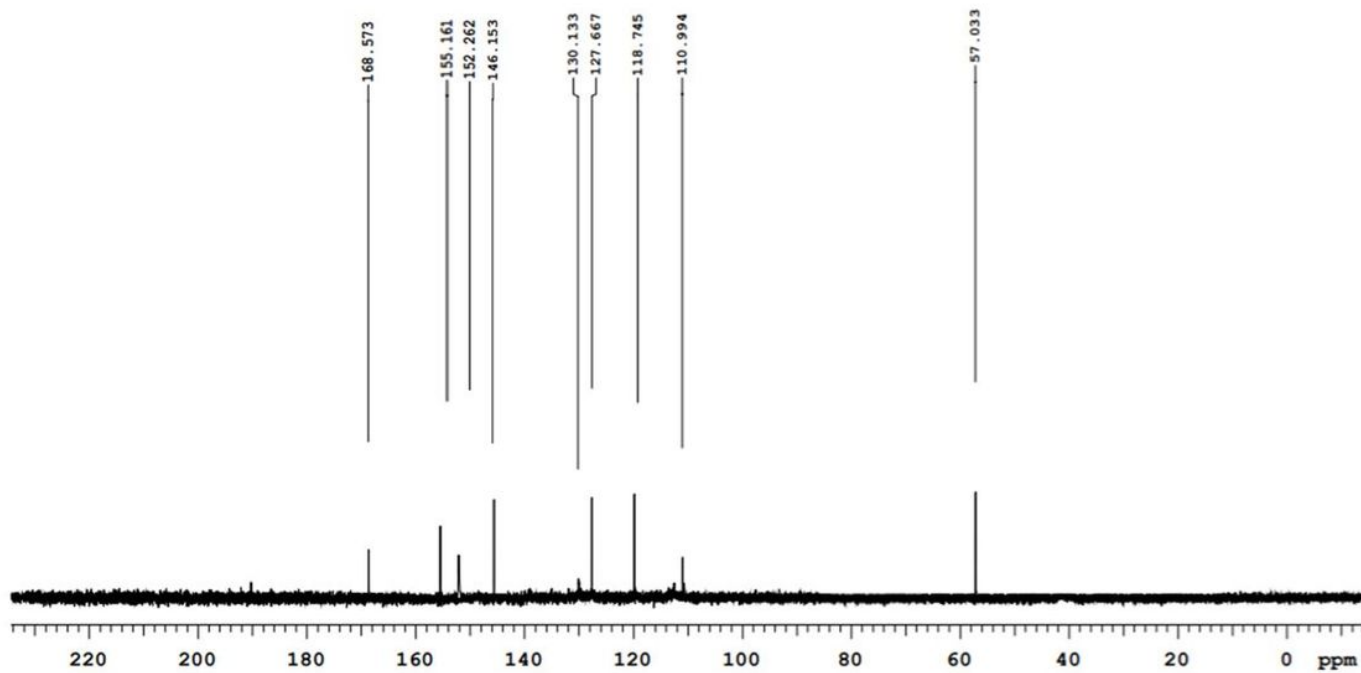


Figure 6

<sup>13</sup>C NMR spectrum of ligand.

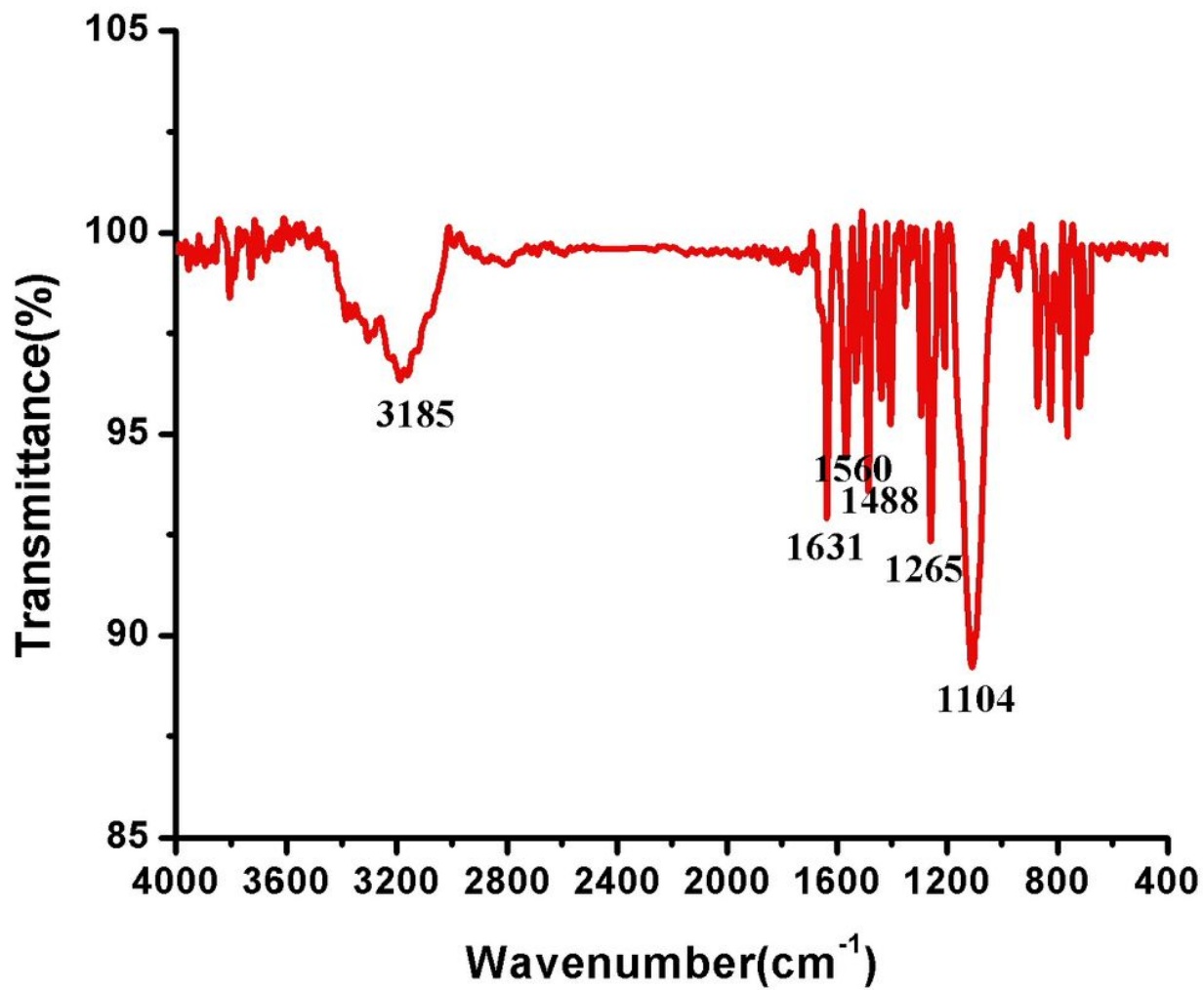


Figure 7

IR spectrum of the Schiff base ligand.

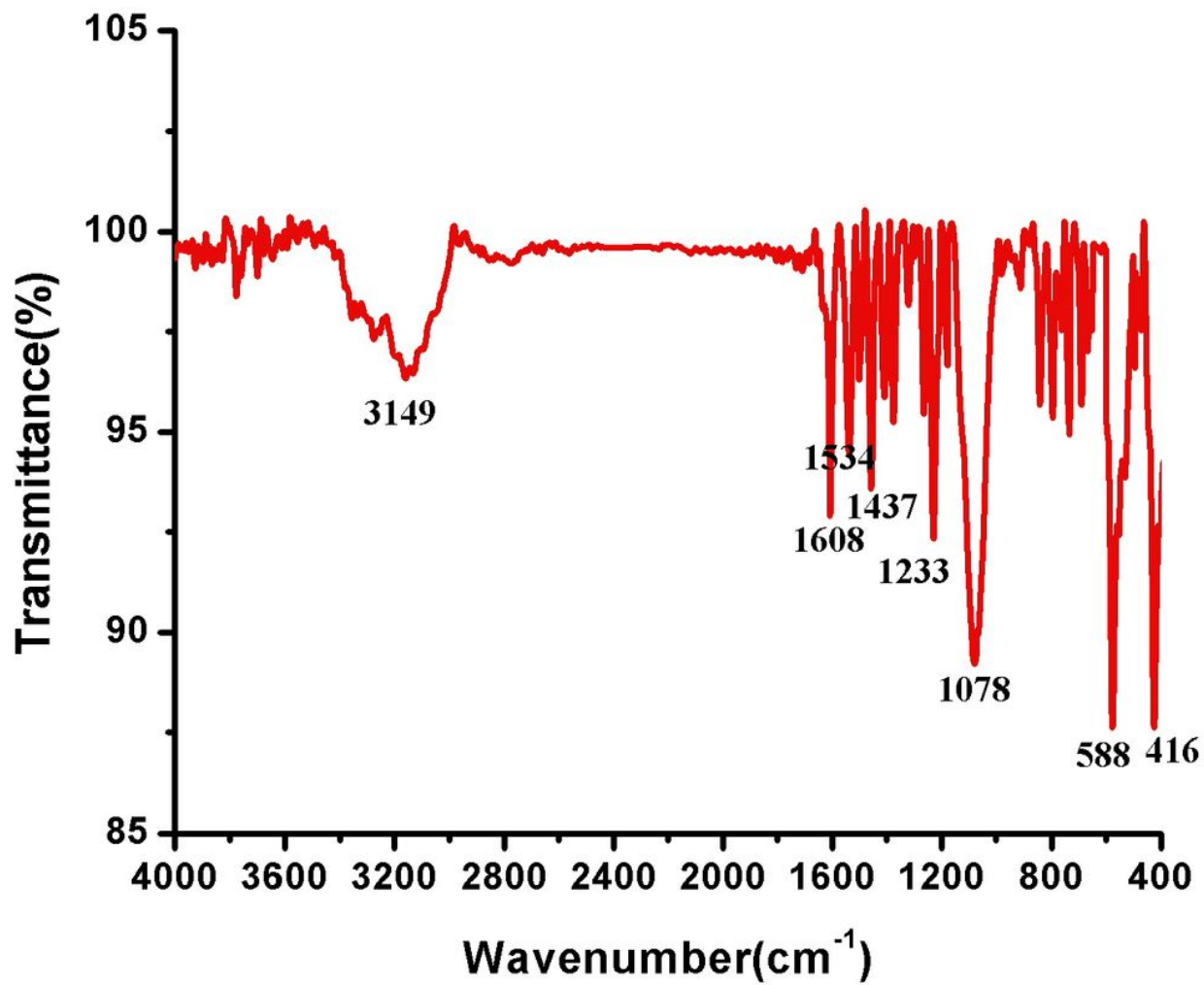


Figure 8

IR spectrum of the Cu(II) complex.

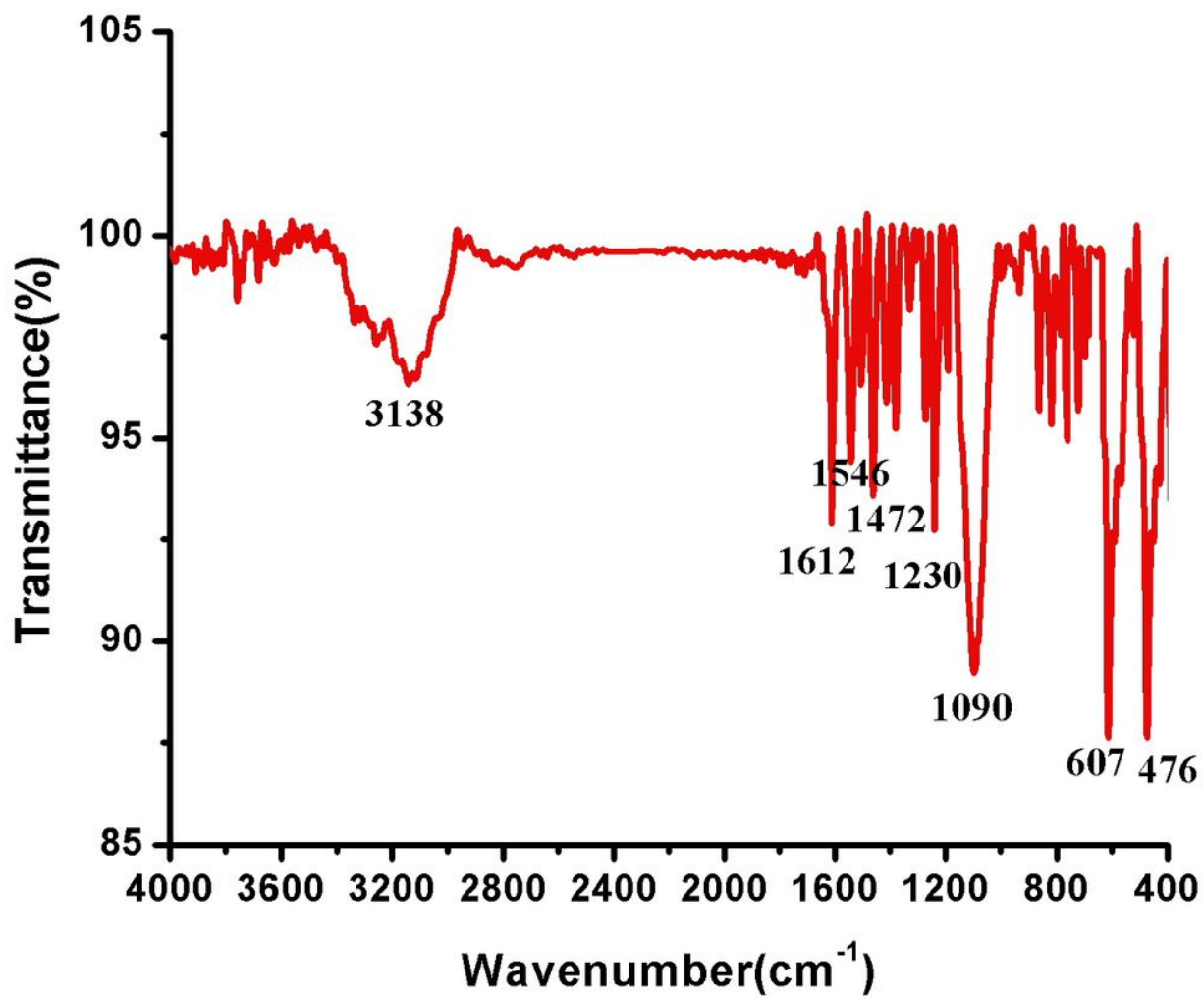


Figure 9

IR spectrum of the Mn(II) complex.

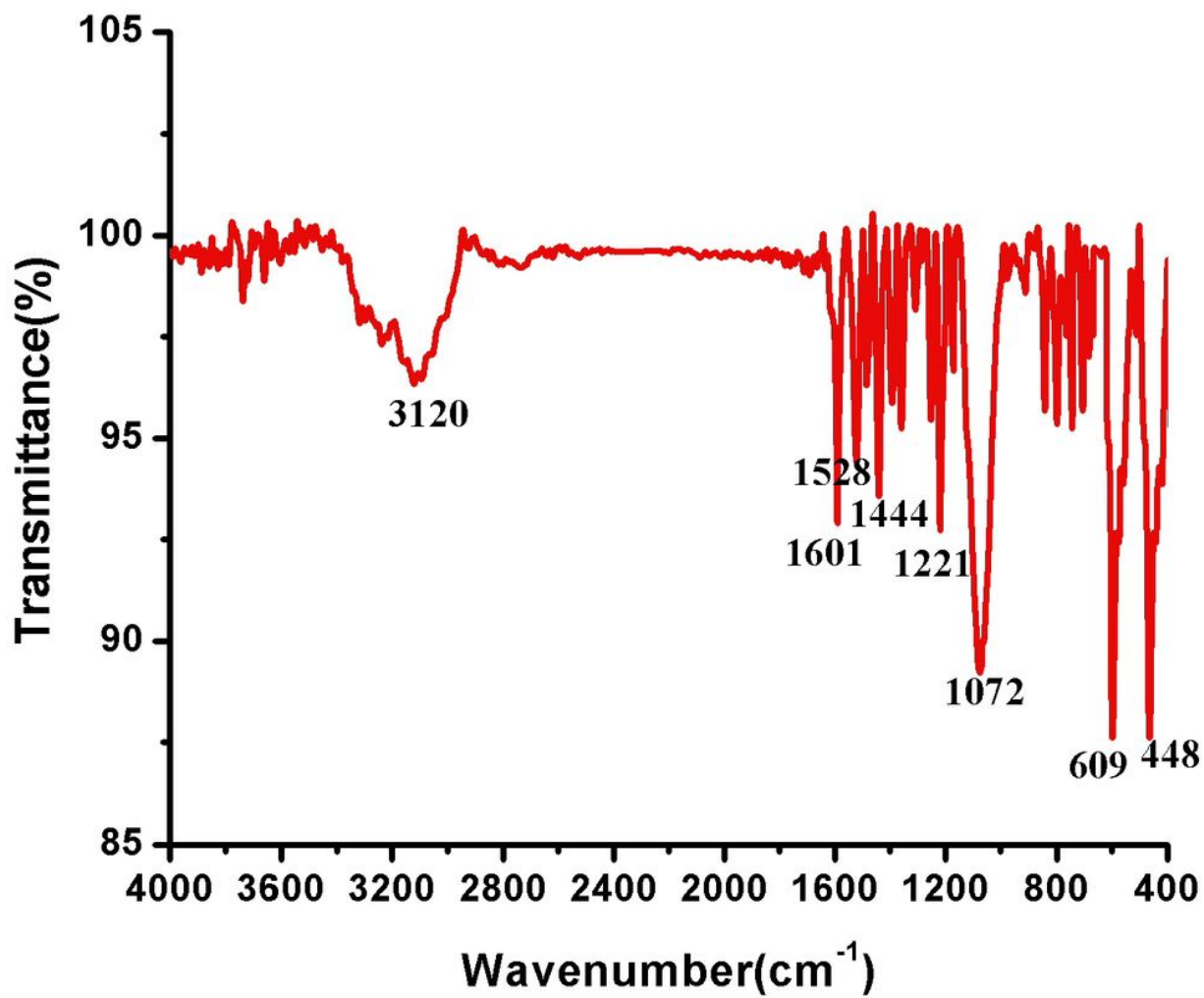


Figure 10

IR spectrum of the Zn(II) complex.

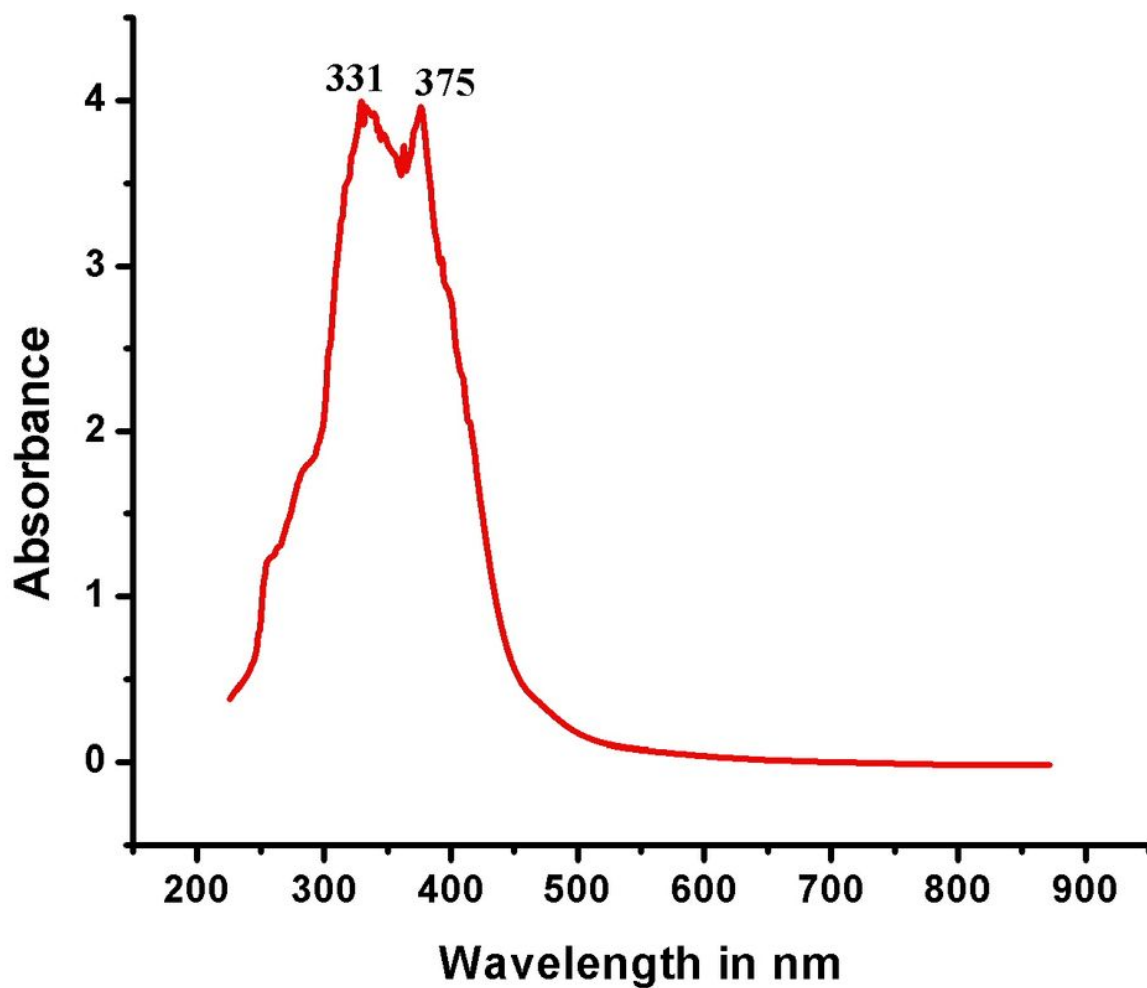


Figure 11

Electronic spectrum of the Schiff base ligand.

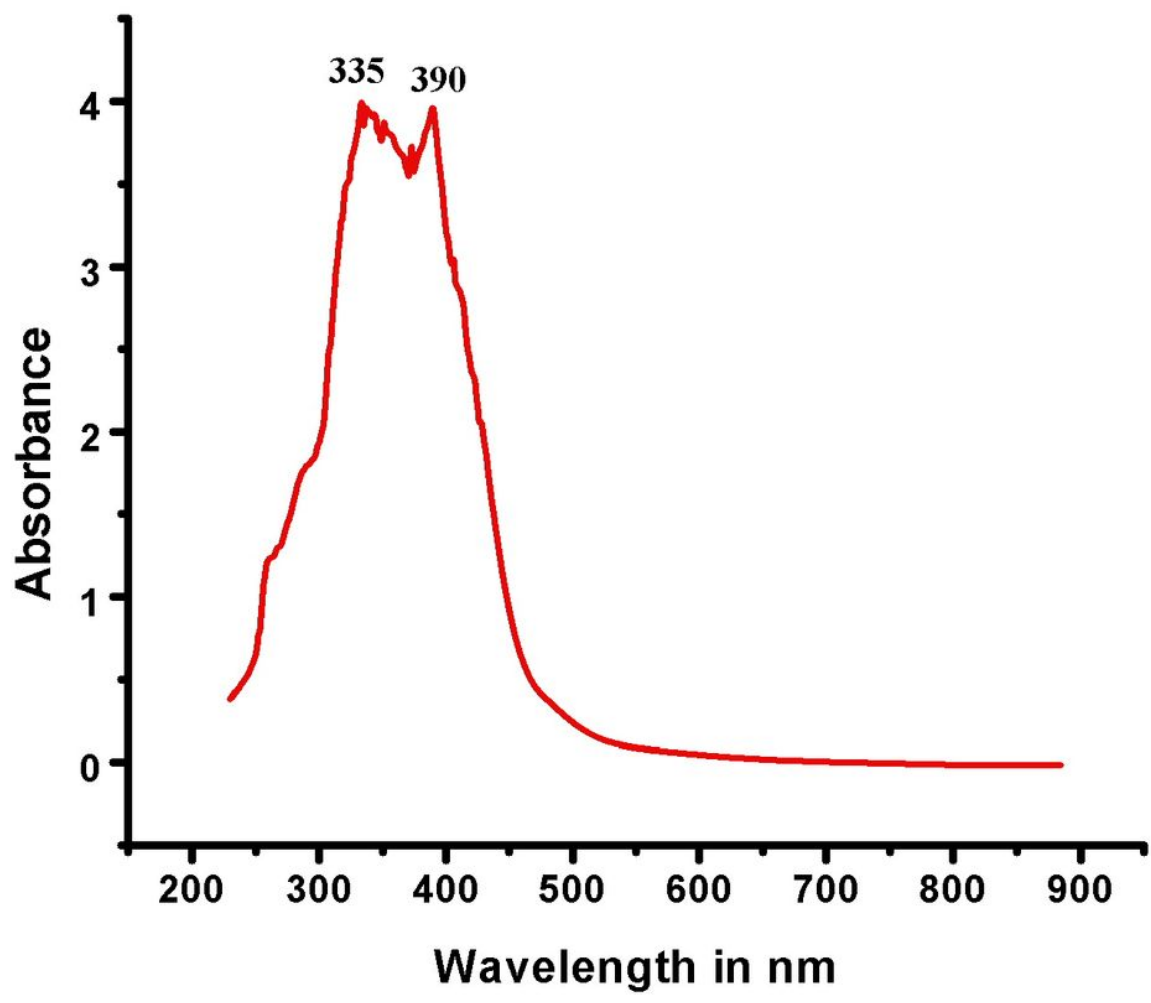


Figure 12

Electronic spectrum of the Cu(II) complex.

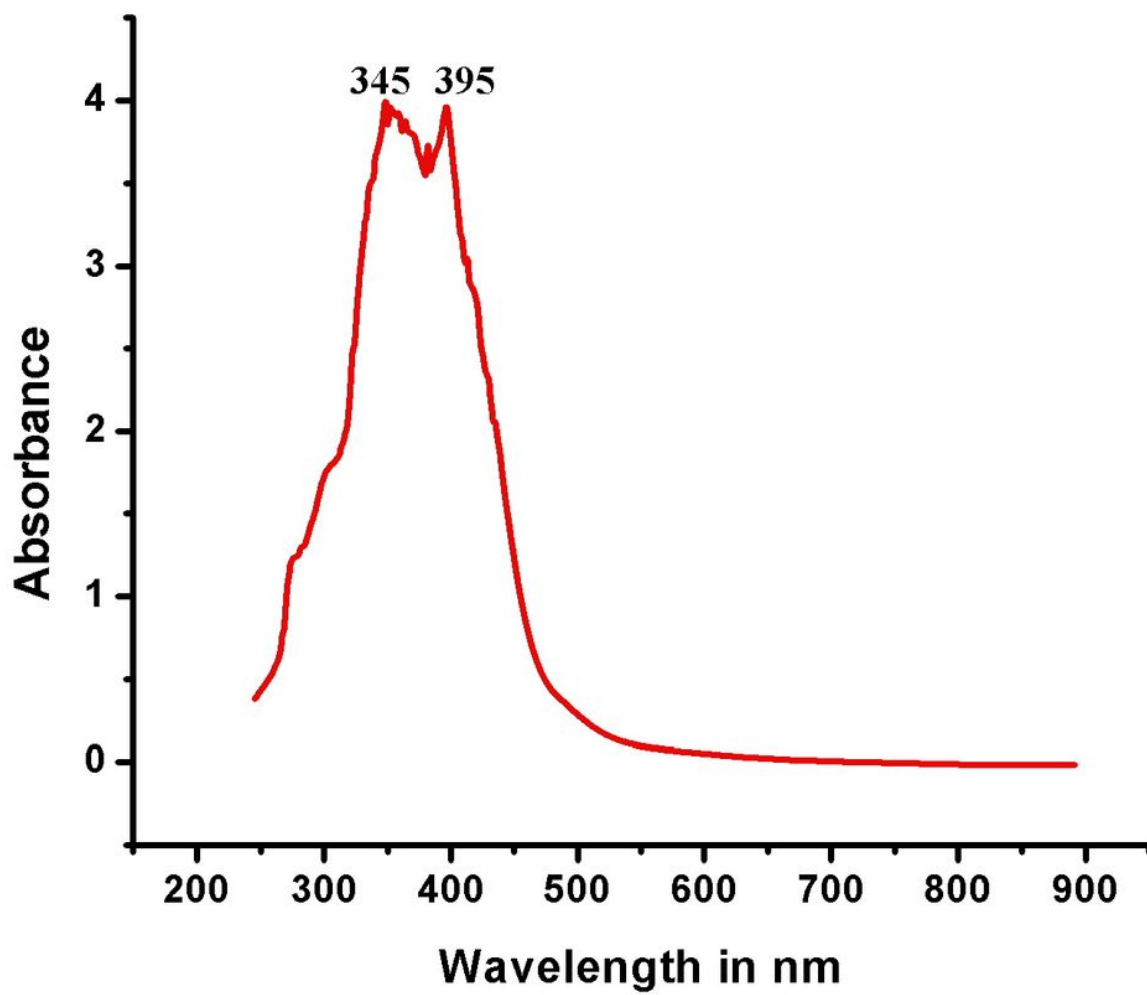


Figure 13

Electronic spectrum of the Mn(II) complex.

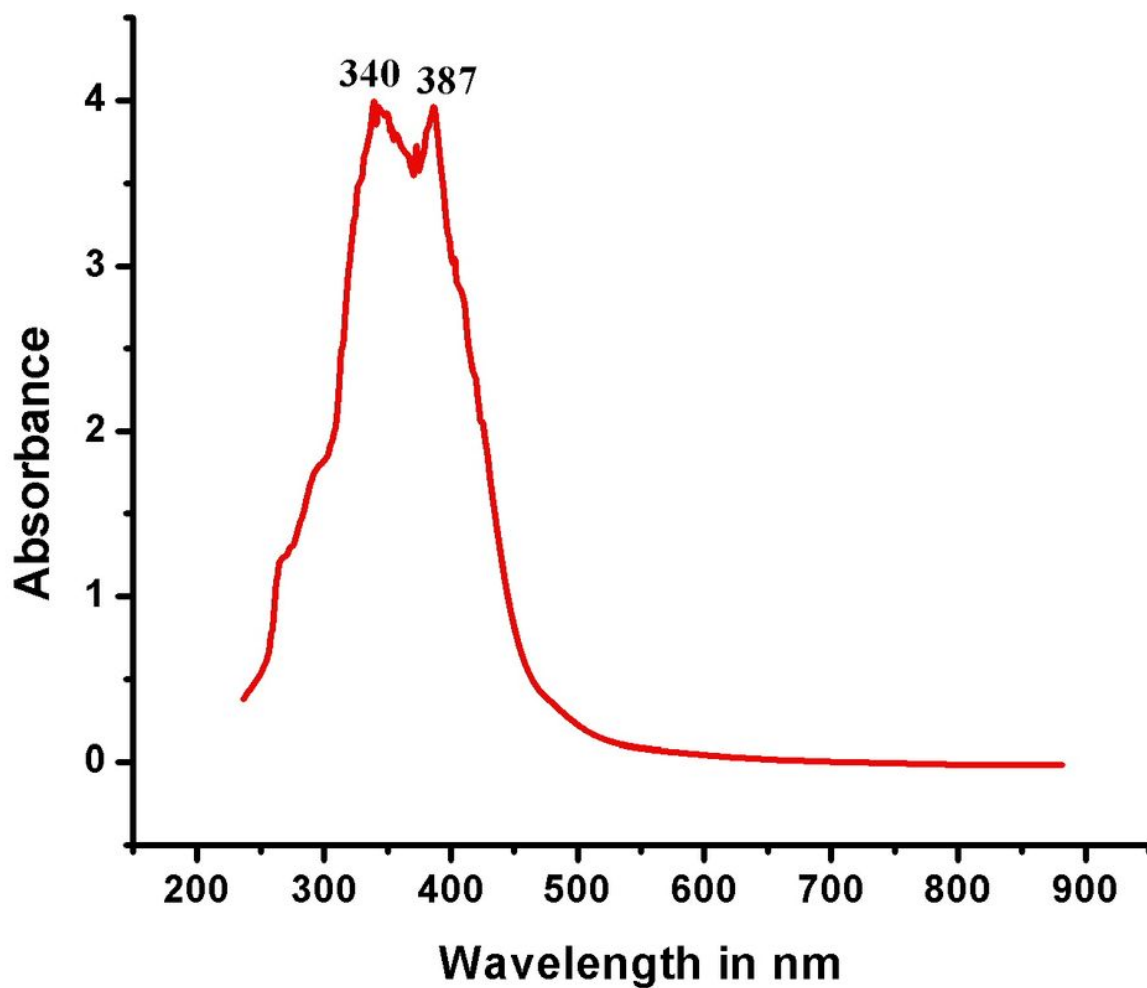


Figure 14

Electronic spectrum of the Zn(II) complex.

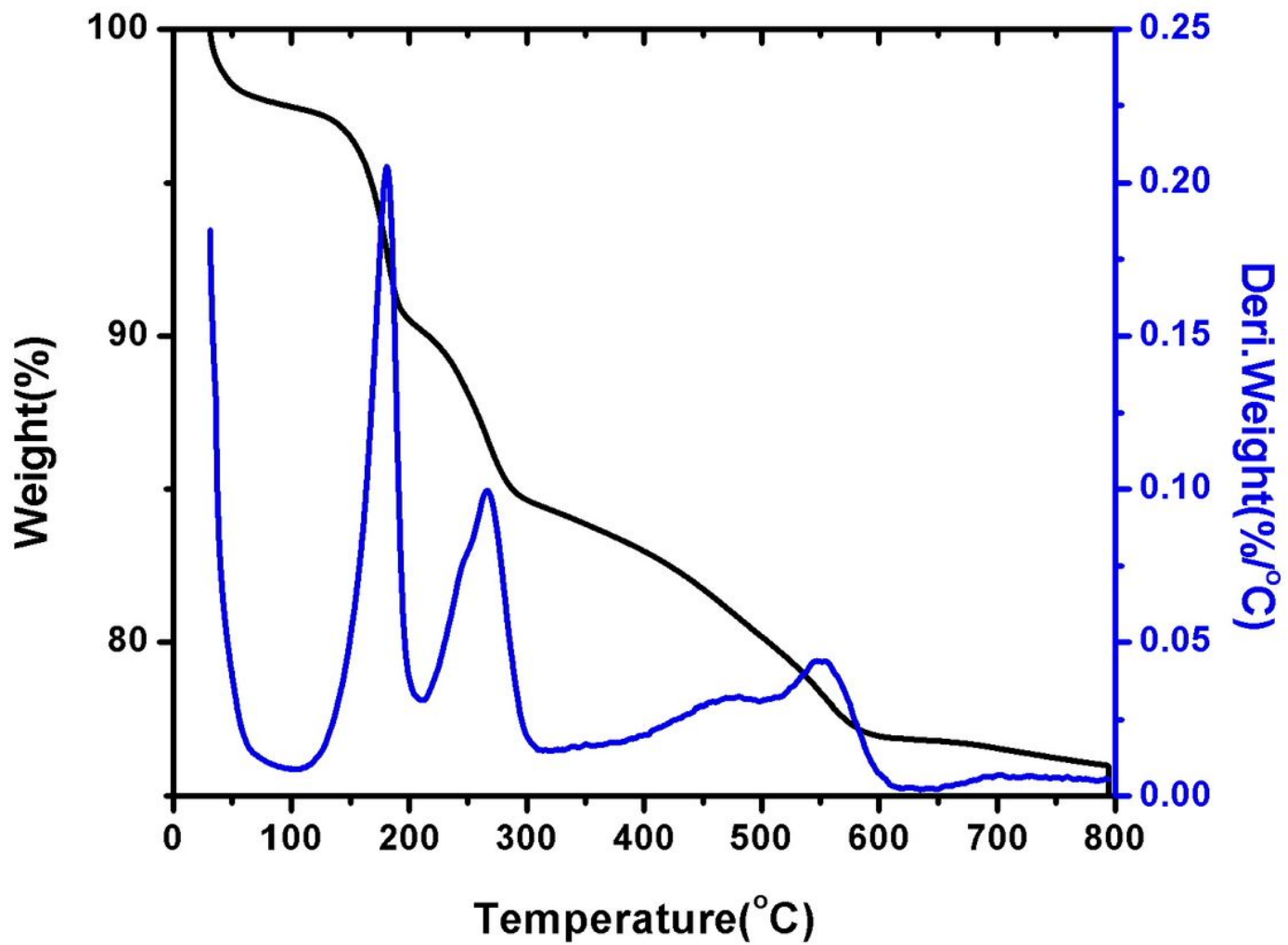


Figure 15

TGA curve of Cu(II) complex .

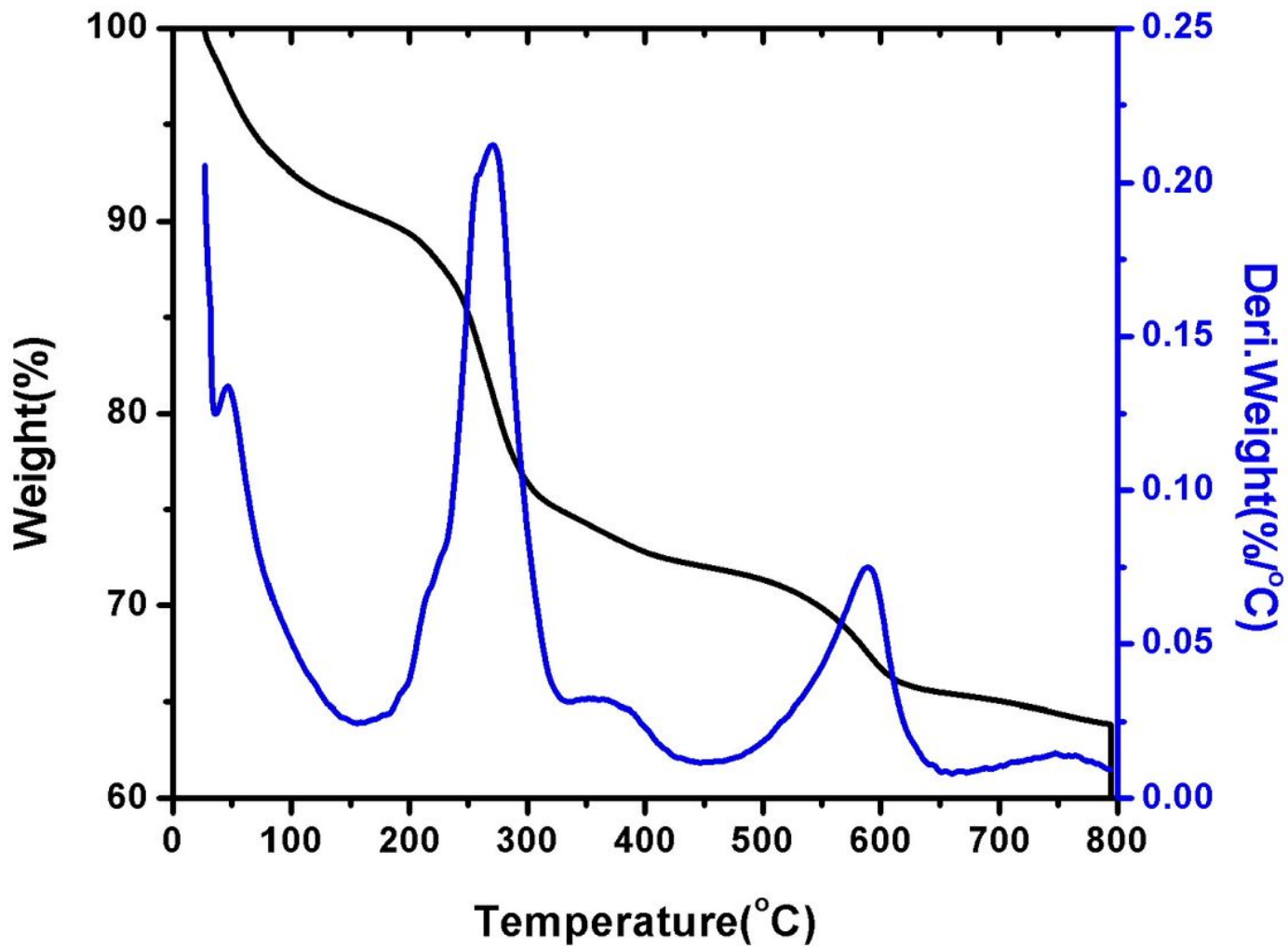


Figure 16

TGA curve of Mn(II) complex.

Image not available with this version

Figure 17

TGA curve of Zn(II) complex.

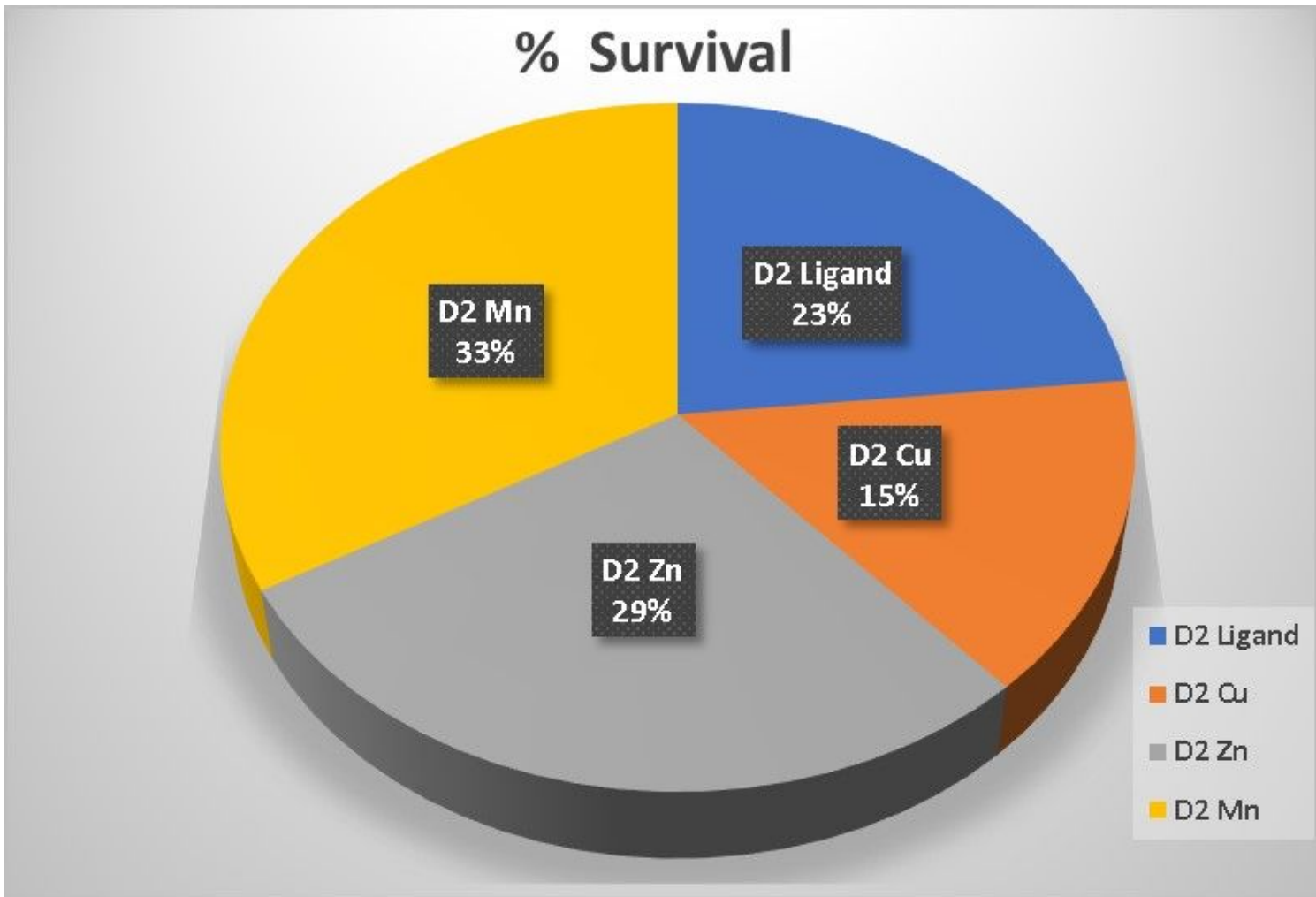


**Figure 18**

% of survival larvicidal activity



Figure 19

larvicidal activity of synthesized compounds

## Supplementary Files

This is a list of supplementary files associated with this preprint. Click to download.

- [Onlinefloatimage1.png](#)